**(Supplementary information)**

# Gas Storage and Separation in Water-Stable $[Cu^{I}_{5}BTT_{3}]^{4-}$ Anion Framework Comprising Giant Multi-prismatic Nanoscale Cage

B. X. Dong,*[a] S. Y. Zhang,[a] W. L. Liu,[a] L. Chen,[a] J. Ge,[a] L. Song[a] and Y. L. Teng*[a]

*College of Chemistry and Chemical Engineering, Yangzhou University, Yangzhou, 225002, P. R. China. Fax: +86 51487975590-9201; Tel: +86 51487975590-9201; E-mail: bxdong@yzu.edu.cn (B-X. Dong); ylteng@yzu.edu.cn (Y-L. Teng).*

## Contents:

## General Procedures.

All chemicals purchased were of reagent grade and were used as received. $H_3BTT$ was synthesized according to a documented procedure.[1] FT-IR spectrum (KBr pellets) was recorded in range of 4000−400 $cm^{-1}$ on a BRUKER TENSOR 27 Fourier-transform infrared spectrometer. TGA/DSC measurement (TGA, Thermal gravimetric analyses; DSC, Differential Scanning Calorimetry) were performed on a TG/DSC Model STA 449 F3 Netzsch instrument at a ramp rate of 5 ºC $min^{-1}$, by heating the sample under argon. Powder XRD data were collected with CuKα (λ=1.5406 Å) radiation on a Bruker-AXS D8 Advance X-ray diffractometer in the angular range 2θ =5°−50° at 296 K. Each pattern is recorded with a 2 s per step scan.

**Synthesis of $[NC_2H_8]_4Cu_5(BTT)_3 \cdot xG$ (G=guest molecule) (1)**

16.0 mL DMA (*N*, *N′*-Dimethylacetamide) solution was added to a beaker, which contains $CuCl_2 \cdot 2H_2O$ (0.068 g, 0.4 mmol) and $H_3BTT \cdot 2HCl$ (0.071 g, 0.2 mmol) with stirring for 30 min. Then the mixture was transferred and sealed in a 23 mL Teflonlined stainless steel container, and heated at 140 °C for 3 days. After slow cooling to room temperature with the rate of 5 °C $h^{-1}$, brown crystals **1** were collected and washed with DMA. Finally, the resulting crystals were dried in a vacuum oven at 80 °C for further treatment and characterization (yield: ca.40.6 mg, 42.2% based on Cu). Prominent FT-IR peaks for **1** (KBr Pellet, $cm^{-1}$): 3379(w), 3059(w), 2781(m), 2472(m), 1663(s), 1610(s), 1465(m), 1414(s), 1259(w), 1099(m), 1020(m), 899(m), 794(s).

## I. X-ray Crystallographic Study

Single-crystal X-ray diffraction analysis data was collected on a Bruker Smart Apex II CCD diffractometer with Mo Kα monochromated radiation (λ=0.71073 Å) at 296 K. All absorption corrections were performed by using the SADABS program. The structure was solved by direct methods and refined on $F^2$ by full-matrix least-squares methods using the SHELXTL package.[2] Anisotropic thermal parameters were used to refine all Cu, C and N atoms. After locating and refining the framework and the counter ions, the difference Fourier map showed many peaks of very low

electronic density, suggesting an extensive disordered of the solvent molecules. Thus, the solvent molecules reside in those regions of diffuse electron density were treated by the PLATON/SQUEEZE procedure,[3] which suggested a unit cell accessible volume of 12836.4 Å$^3$ (about 40.5%). The hydrogen atoms attached to carbon positions were placed in geometrically calculated positions. The crystal data and structure refinement results of squeezed compound **1** are summarized in Table S1. Selected bond lengths and angles are listed in Tables S2. Atomic coordinates and equivalent isotropic displacement parameters are listed in Table S3. Valence bond calculations for the three independent Cu centers in each asymmetric unit are listed in Table S4. Crystallographic data for the structure reported in this paper has been deposited in the Cambridge Crystallographic Data Center with CCDC number 1034129 for **1**.

```
:: Resd  1 - Infinite (Type1) 3D-Framework: Det = 1
:: Base Vectors:     1 :   1  1  0 ,     2 :   0  1 -1 ,     3 :   2  1  0 ,
:: Resd  1, SOF 1.000, Z 16, C27 H9 Cu5 N36
:: Resd  2, SOF 1.000, Z 32, C2 H8 N
:: Resd  3, SOF 1.000, Z 32, C2 H8 N
:: Moiety_Formula = C27 H9 Cu5 N36, 4(C2 H8 N)
:: Sum_Formula    = C35 H41 Cu5 N40
:: Formula_Weight =     1339.83 [Note: Based on SHELXL2014 Atomic Weights]
:: Formula_Z      =          16
:: SpaceGroup_Z   =          32
:: Formula_Z'     =       0.500
:: mu(MoKa)       =       13.68 cm-1 =   1.368 mm-1
:: Predicted Vol  =     20803.7[   20799.7] Ang**3, 298[296]K
:: ADP  N1        0.024   0.030   0.215 - RATIO(MAX/MIN) =      9.0 prolate
:: ADP  N11       0.018   0.046   0.203 - RATIO(MAX/MIN) =     11.1 prolate
:: ADP  N12       0.021   0.036   0.209 - RATIO(MAX/MIN) =     10.0 prolate
:: ADP  C20       0.123   0.385   1.267 - RATIO(MAX/MIN) =     10.3 prolate
:: ADP  N21       0.099   0.202   1.061 - RATIO(MAX/MIN) =     10.7 prolate

:: VOID/SOLV Gridstep (Angstrom) (re)set to 0.20, Percent Memory =  4.1

van der Waals (or ion) Radii used in the Analysis
================================================================================
    C    H   Cu    N    O
--------------------------------------------------------------------------------
 1.70 1.20 1.40 1.55 1.52
:: Note: VOID/SOLV/SQUEEZE is relatively compute intense and experimental

:: Total Potential Solvent Area Vol  12836.4 Ang^3
                 per Unit Cell Vol  31702.0 Ang^3 [40.5%]

Note: Expected volumes for solvent molecules are:
      A hydrogen bonded H2O-molecule      40 Ang^3
      Small molecules (e.g. Toluene) 100-300 Ang^3

      Values below for gridpoints and volumes in []
      refer to areas where atom centers may reside.

:: Use the CALC SQUEEZE instruction to calculate and optionally correct for
:: Density identified in solvent accessible areas (Reflection data required)
```

Calculation result of PLATON/SQUEEZE.

## II. Gas Sorption Measurements

In the gas sorption measurement, Ultra-high-purity grade $N_2$, He, $H_2$, $CO_2$ (>99.999% purity) and $CH_4$ (>99.995% purity) gases were used throughout the adsorption experiments. All of the measured sorption isotherms have been repeated several times to confirm the reproducibility within experimental error.

**Low-Pressure Gas Sorption Measurements**

Low-pressure $N_2$ adsorption measurements (up to 1 bar) were performed on a Micromeritics ASAP 2020 HD88 surface area and pore size analyzer. About 200 mg of acetone solvent-exchanged sample was degassed at 40 $^oC$ at the "degassing station" of ASAP 2020 surface area and porosity analyzer under dynamic high vaccum (oil pump) for 24 h and then at "analyzing station" under turbine molecular pump for 12 h. High vacuum was maintained at a pressure < 1 μm Hg after 8 hours degassing at "degassing station" and was maintained at a pressure < 0.05 μm Hg for the final 8 hours activation at the "analyzing station". Helium was used for the estimation of the dead volume, assuming that it is not adsorbed at any of the studied temperatures. A part of the $N_2$ sorption isotherm in the $P/P_0$ range 0.005−0.05 was fitted to the BET equation to estimate the BET surface area[4] and the Langmuir surface area calculation was performed using all data points.[5]

**High-Pressure Gravimetric Gas Sorption Measurements**

High-pressure excess adsorption isotherms of $CO_2$, $H_2$ and $N_2$ were measured on a Rubotherm MSB (magnetic suspension balance) apparatus by the gravimetric method. About 120 mg fully desolvated samples were used for high-pressure sorption measurements. The significance of the balance is ≤0.1 mg. Thus, a stainless steel sample holder was filled with the fully desolvated sample and the balance was evacuated for 24 h until constant mass was achieved. Afterwards, the gas was dosed into the balance chamber to elevated pressure. Equilibrium was achieved within 30 min and identified by constant weight and pressure. The temperature was kept constant with an accuracy of ±0.5 K for each measurement. The total gas uptake was calculated using the following equation,[6]

$$N_{\text{total}} = N_{\text{excess}} + \frac{100 \times V_{\text{pore}} \times \rho_{\text{gas}}}{(1 + V_{\text{pore}} \times \rho_{\text{gas}})} \quad (1)$$

where $N_{\text{total}}$ is the total uptake amount of gas (wt%), $N_{\text{excess}}$ is the surface excess uptake amount of gas (wt%), $V_{\text{pore}}$ is the crystallographic pore volume (0.302 $cm^3\ g^{-1}$ in this work) which is determined from the nitrogen isotherm, and $\rho_{\text{gas}}$ (g $cm^{-3}$) is the density of the compressed gas as a function of pressure at certain temperature.[7]

## III. Isosteric Heat of Adsorption ($Q_{st}$) Calculations

A virial-type[8] expression comprising the temperature-independent parameters $a_i$ and $b_i$ was employed to calculate the enthalpies of adsorption for $CO_2$ (at 273 and 298 K) on **1a**. In each case, the data were fitted using the equation:

$$\ln P = \ln N + 1/T \sum_{i=0}^{m} a_i N^i + \sum_{j=0}^{n} b_j N^j \quad (2)$$

Here, $P$ is the pressure expressed in Torr, $N$ is the amount adsorbed in mmol $g^{-1}$, $T$ is the temperature in K, $a_i$ and $b_i$ are virial coefficients, and $m$, $n$ represent the number of coefficients required to adequately describe the isotherms ($m$ and $n$ were gradually increased until the contribution of extra added $a$ and $b$ coefficients was deemed to be statistically insignificant towards the overall fit, and the average value of the squared deviations from the experimental values was minimized). The values of the virial coefficients $a_0$ through $a_m$ were then used to calculate the isosteric heat of adsorption using the following expression:

$$Q_{st} = -R \sum_{i=0}^{m} a_i N^i \quad (3)$$

$Q_{st}$ is the coverage-dependent isosteric heat of adsorption and $R$ is the universal gas constant. The heat of $CO_2$ sorption for **1a** in this manuscript is determined by using the excess sorption data measured in the pressure range from 0−800 mmHg (273 and 298 K), which is fitted by the virial-equation very well ($R^2$>0.999).

## IV. Prediction of the Gases Adsorption Selectivity by IAST

IAST (ideal adsorption solution theory)[9] was used to predict binary mixture

adsorption from the experimental pure-gas isotherms. In order to perform the integrations required by IAST, the single-component isotherms should be fitted by a proper model. In practice, several methods to do this are available. For $N_2$/**1a** in the low pressure, the single-site Langmuir model (SSL),[10]

$$q = \frac{q_{sat} bP}{1 + bP} \qquad (4)$$

was used for isotherm fitting. Where, $b$ is the parameter in the pure component Langmuir isotherm ($Pa^{-1}$), $P$ is the pressure of the bulk gas at equilibrium with the adsorbed phase $P$ (Pa), $q$ is the adsorbed amount of adsorbent (mol $kg^{-1}$), $q_{sat}$ is saturation capacity of species (mol $kg^{-1}$).

The situations with $CO_2$/**1a** and $H_2$/**1a** in low pressure are different and a similar approach to the above using single-site Langmuir model fits is inadequate. We found for these sets of data that the dual-site Langmuir-Freundlich equation (DSLF)[10-12] was successful in fitting the data:

$$q = \frac{q_{m,1} b_1 P^{1/n_1}}{1 + b_1 P^{1/n_1}} + \frac{q_{m,2} b_2 P^{1/n_2}}{1 + b_2 P^{1/n_2}} \qquad (5)$$

Here, $p$ is the pressure of the bulk gas at equilibrium with the adsorbed phase (Pa), $q$ is the adsorbed amount of adsorbent (mol $kg^{-1}$), $q_{m,1}$ and $q_{m,2}$ are the saturation capacities of sites 1 and 2 (mol $kg^{-1}$). $b_1$ and $b_2$ are the affinity coefficients of sites 1 and 2 ($Pa^{-1}$), and $n_1$ and $n_2$ represent the deviations from an ideal homogeneous surface.

Pure-component isotherm fitting parameters were then used for calculating IAST binary-gas adsorption selectivities, $S_{A/B}$, defined as:

$$S_{A/B} = \frac{q_A / q_B}{P_A / P_B} \qquad (6)$$

## V. Gas Cycling Mesurements.

$CO_2$ cycling experiments were performed on a TG/DSC Model STA 449 F3 Netzsch instrument. A flow of 15% (v/v) $CO_2$ mixture in $N_2$ was applied followed by

a stream of pure $N_2$ (>99.999%). The flow rates for pure $N_2$ gas and $CO_2$–$N_2$ (15:85 v/v) mixture gas are 60 mL $min^{-1}$ and 40 mL $min^{-1}$, respectively.

Table S1. Crystal data and structure refinement for compound **1**.

| Compound | **$[NC_2H_8]_4C_{27}H_9Cu_5N_{36}$** |
|---|---|
| Empirical formula | $C_{35}H_{41}Cu_5N_{40}$ |
| Formula weight | 1339.78 |
| Temperature (K) | 296(2) |
| Wavelength (Å) | 0.71073 |
| Crystal system | Orthorhombic |
| Space group | *Fddd* |
| a/Å | 16.180(2) |
| b/Å | 43.077(5) |
| c/Å | 45.485(6) |
| V/Å$^3$ | 31702(7) |
| Z | 16 |
| $D_{calc}$ (Mg/m$^3$) | 1.123 |
| Absorption coefficient (mm$^{-1}$) | 1.368 |
| F(000) | 10816 |
| θ range for data collection | 1.417 to 24.999 deg |
| Reflections collected / unique | 68507 / 7000 [R(int) = 0.0840] |
| Limiting indices | -19<=h<=19, -49<=k<=51, -54<=l<=54 |
| Completeness to θ= 25.242 | 97.4 % |
| Goodness-of-fit on $F^2$ | 0.993 |
| Final R indices [I>2sigma(I)] | *R1 = 0.0489, wR2 = 0.1360* |
| R indices (all data) | *R1 = 0.0853, wR2 = 0.1474* |
| Largest diff. peak and hole (e. Å$^{-3}$) | 0.588 and -0.409 |
| *Total potential solvent area Vol* Å $^3$ *per Unit Cell Vol 31702.0* Å $^3$ | 12836.4 (40.5%) |

Table S2. Selected bond distances (Å) and angles (°) for **1**.

| | | | |
|---|---|---|---|
| Cu(1)-N(18) | 2.069(2) | N(18)-Cu(1)-N(4)#1 | 104.2(3) |
| Cu(1)-N(18)#1 | 2.070(7) | N(18)#1-Cu(1)-N(4)#1 | 119.3 (3) |
| Cu(1)-N(4) | 2.068(2) | N(4)-Cu(1)-N(4)#1 | 99.9 (3) |
| Cu(1)-N(4)#1 | 2.068(7) | N(3)-Cu(2)-N(14) | 113.91(13) |
| Cu(2)-N(3) | 1.978(2) | N(3)-Cu(2)-N(5) | 114.92(11) |
| Cu(2)-N(14) | 2.010(3) | N(14)-Cu(2)-N(5) | 114.57(10) |
| Cu(2)-N(5) | 2.064(2) | N(3)-Cu(2)-N(17) | 113.78(10) |
| Cu(2)-N(17) | 2.097(2) | N(14)-Cu(2)-N(17) | 99.74(12) |
| Cu(3)-N(6) | 1.963(2) | N(5)-Cu(2)-N(17) | 97.70(11) |
| Cu(3)-N(13) | 2.063(3) | N(6)-Cu(3)-N(13) | 107.84(10) |
| Cu(3)-N(9)#2 | 2.071(4) | N(6)-Cu(3)-N(9)#2 | 129.71(12) |
| Cu(3)-N(10) | 2.071(4) | N(13)-Cu(3)-N(9)#2 | 99.84(13) |
| N(18)-Cu(1)-N(18)#1 | 110.3(3) | N(6)-Cu(3)-N(10) | 120.02(15) |
| N(18)-Cu(1)-N(4) | 119.26(9) | N(13)-Cu(3)-N(10) | 97.75(13) |
| N(18)#1-Cu(1)-N(4) | 104.3(3) | N(9)#2-Cu(3)-N(10) | 95.98(17) |
| Symmetry transformations used to generate equivalent atoms:<br>#1 -x+5/4,y,-z+1/4 #2 -x+3/4,-y+3/4,z | | | |

Table S3. Atomic coordinates ($\times 10^4$) and equivalent isotropic displacement parameters (Å $\times 10^3$) for compound **1**. $U_{(eq)}$ is defined as one third of the trace of the orthogonalized $U_{ij}$ tensor.

| | x | y | z | U(eq) |
|---|---|---|---|---|
| Cu(1) | 6250 | 4278(1) | 1250 | 32(1) |
| Cu(2) | 5013(1) | 4288(1) | 624(1) | 34(1) |
| Cu(3) | 4315(1) | 4080(1) | -105(1) | 42(1) |
| C(1) | 4987(3) | 4823(1) | 1360(1) | 46(1) |
| C(2) | 5334(3) | 4957(1) | 1636(1) | 44(1) |
| C(3) | 5824(3) | 4786(1) | 1826(1) | 39(1) |
| C(4) | 6114(2) | 4918(1) | 2086(1) | 35(1) |
| C(5) | 5887(3) | 4741(1) | 197(1) | 35(1) |
| C(6) | 5914(3) | 5222(1) | 2151(1) | 45(1) |
| C(7) | 5426(3) | 5394(1) | 1959(1) | 50(1) |
| C(9) | 5127(3) | 5256(1) | 1703(1) | 50(1) |
| C(10) | 3750 | 3750 | 1057(1) | 27(1) |
| C(11) | 3024(3) | 3688(1) | 1211(1) | 35(1) |
| C(12) | 3021(3) | 3688(1) | 1519(1) | 38(1) |
| C(13) | 3750 | 3750 | 1666(1) | 45(2) |
| C(14) | 7251(3) | 3864(1) | 809(1) | 38(1) |
| C(15) | 3750 | 3750 | 733(1) | 26(1) |
| N(1) | 4336(3) | 4946(1) | 1223(1) | 89(2) |
| N(2) | 4237(3) | 4776(1) | 976(1) | 72(1) |
| N(3) | 4806(2) | 4564(1) | 967(1) | 37(1) |
| N(4) | 5287(2) | 4585(1) | 1206(1) | 30(1) |
| N(5) | 5349(2) | 4516(1) | 249(1) | 29(1) |
| N(6) | 5082(2) | 4423(1) | -19(1) | 33(1) |
| N(7) | 5444(2) | 4591(1) | -220(1) | 49(1) |
| N(8) | 5963(2) | 4794(1) | -94(1) | 50(1) |
| N(10) | 4746(3) | 3686(1) | -316(1) | 59(1) |
| N(11) | 5430(3) | 3651(1) | -471(1) | 88(2) |
| N(12) | 5479(3) | 3360(1) | -573(1) | 90(2) |
| N(13) | 3990(2) | 3874(1) | 286(1) | 29(1) |
| N(14) | 4149(2) | 3958(1) | 567(1) | 28(1) |
| N(15) | 7189(3) | 3772(1) | 530(1) | 82(2) |
| N(16) | 6434(3) | 3868(1) | 448(1) | 71(1) |
| N(17) | 6069(2) | 4008(1) | 665(1) | 35(1) |
| N(18) | 6576(2) | 4004(1) | 900(1) | 26(1) |
| N(9) | 4320(2) | 3413(1) | -312(1) | 47(1) |
| C(8) | 4785(3) | 3220(1) | -472(1) | 58(2) |
| C(20) | 8123(18) | 5690(5) | -850(6) | 590(40) |

| | | | | |
|---|---|---|---|---|
| C(21) | 8044(14) | 5664(4) | -280(4) | 319(12) |
| C(22) | 11066(19) | 4392(11) | -1538(11) | 700(40) |
| C(23) | 12749(19) | 4241(8) | -1529(6) | 550(30) |
| N(20) | 8261(13) | 5497(4) | -568(5) | 398(14) |
| N(21) | 11970(20) | 4377(4) | -1662(3) | 450(20) |

Table S4. Valence bond calculations of three crystallographically independent Cu centers in compound **1**.

| | Distance | BVS |
|---|---|---|
| Cu(1)-N(4)$^{\#1}$ | 2.068(7) | ∑(Cu1)=1.21 |
| Cu(1)-N(4) | 2.068(2) | |
| Cu(1)-N(18)$^{\#1}$ | 2.070(7) | |
| Cu(1)-N(18) | 2.069(2) | |
| Cu(2)-N(3) | 1.978(2) | ∑(Cu2)=1.28 |
| Cu(2)-N(14) | 2.010(3) | |
| Cu(2)-N(5) | 2.064(2) | |
| Cu(2)-N(17) | 2.097(2) | |
| Cu(3)-N(6) | 1.963(2) | ∑(Cu3)=1.26 |
| Cu(3)-N(10) | 2.071(4) | |
| Cu(3)-N(13) | 2.057(3) | |
| Cu(3)-N(9) | 2.071(4) | |

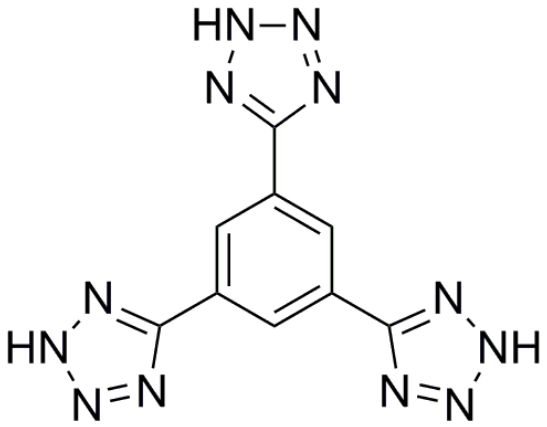


Figure S1. The structure of the $H_3$BTT ligand.

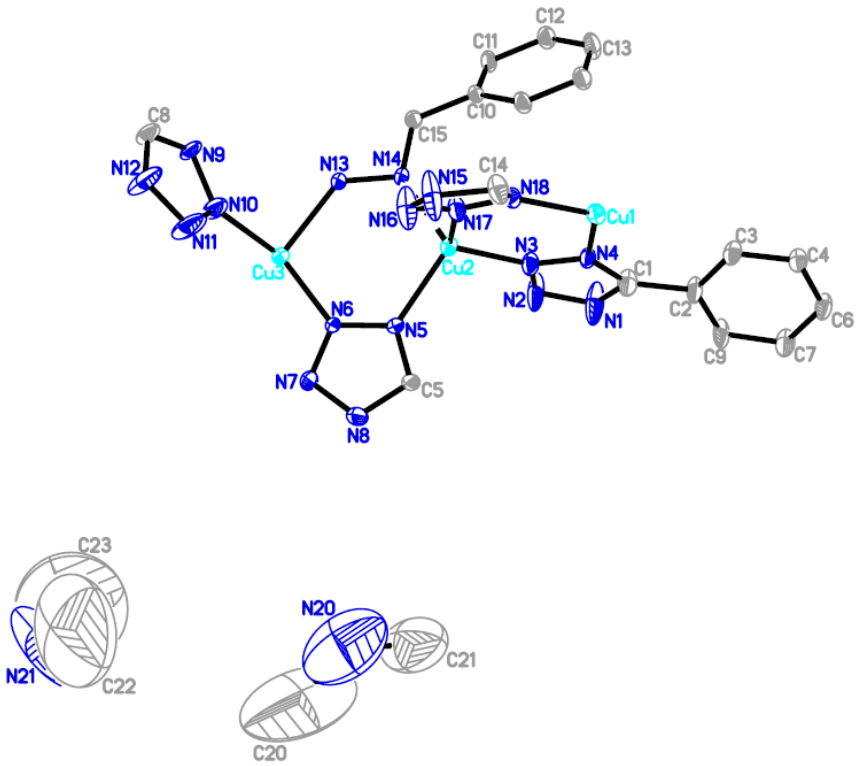


Figure S2. Ortep drawing of the asymmetric unit of the compound **1** after PLATON/SQUEEZE treatment.

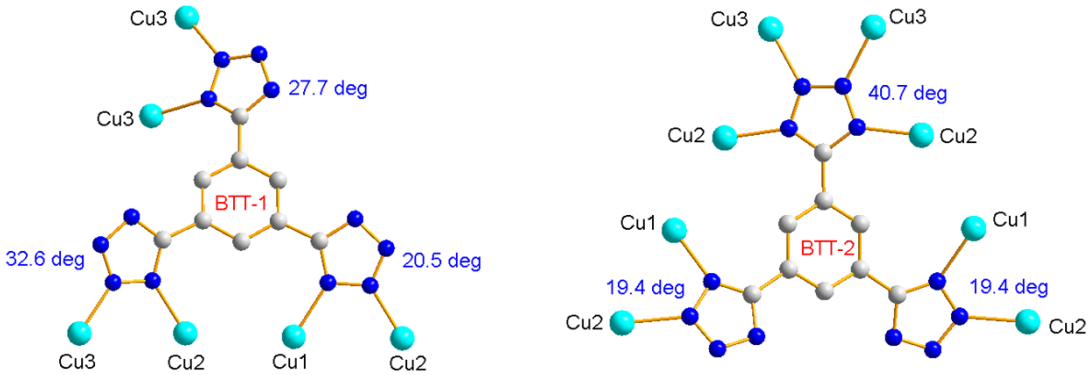


(a) (b)

Figure S3. Representations of the (a) $\mu_6$-btt$^{3-}$ and (b) $\mu_8$-btt$^{3-}$ ligand, as well as the angles between planes in these two BTT ligands.

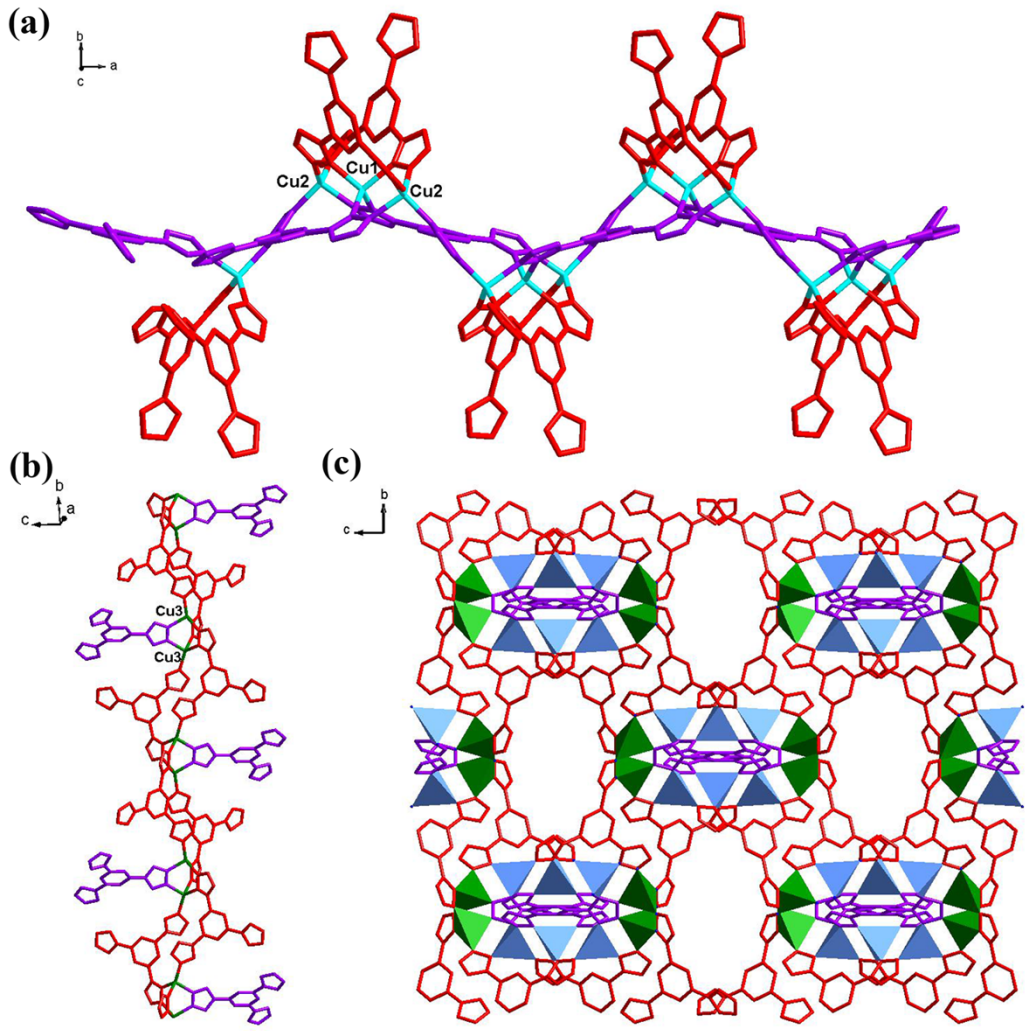


Figure S4. View of the 1D chain constructed by the tri-nuclear $Cu_3$ clusters (a) and bi-nuclear $Cu_2$ clusters (b); (c) View of the 3D open anion framework of **1** embedded with meso-helical chains.

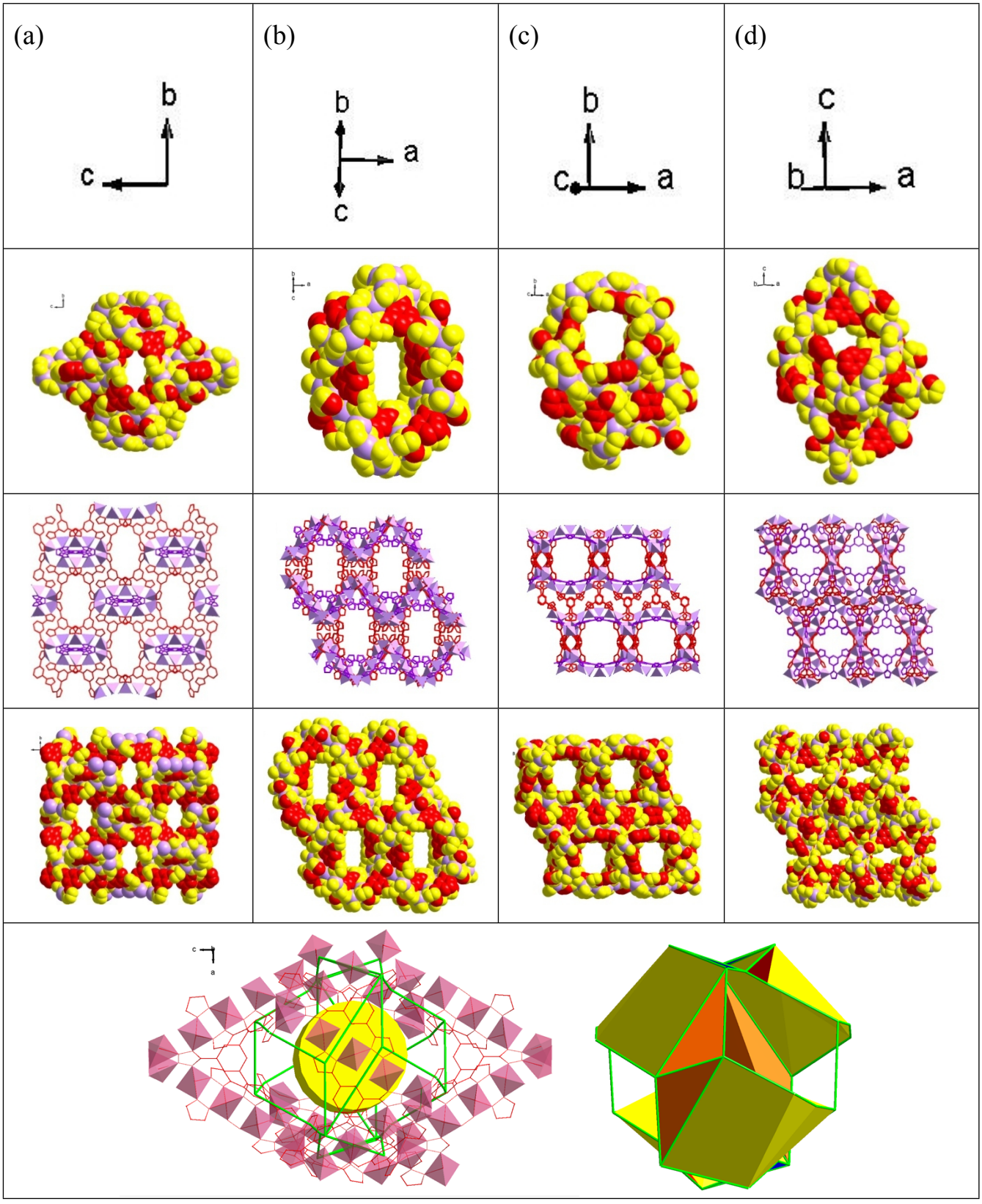


Figure S5. Representations of the four types of channels (a-d) and the giant cavity (e) in compound **1**.

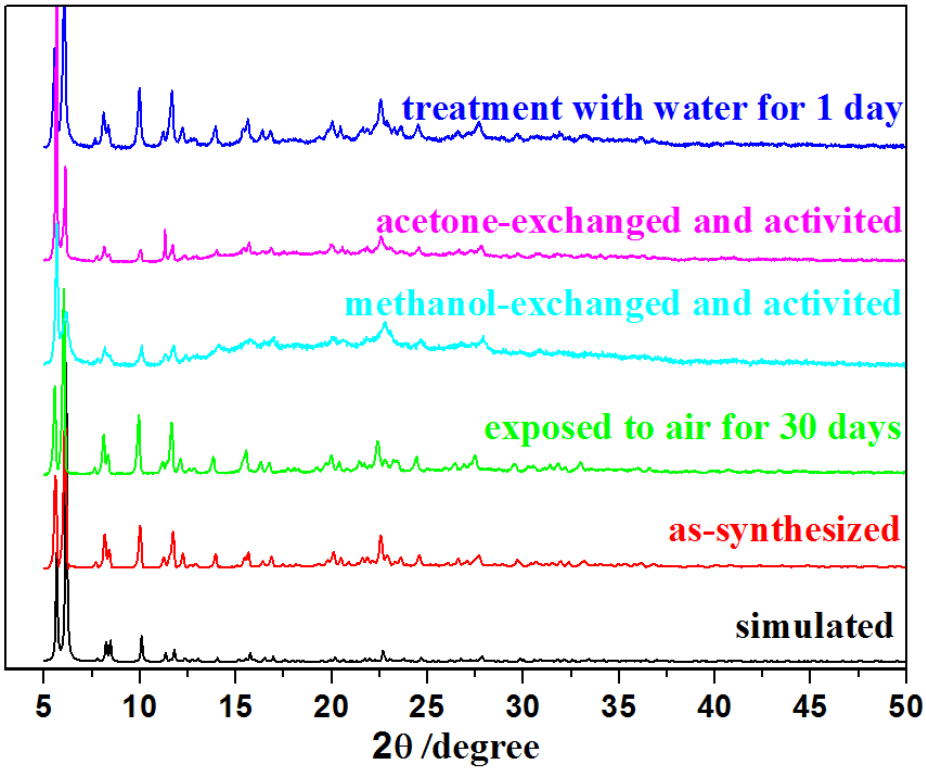


Figure S6. The PXRD patterns for compound **1** after different test.

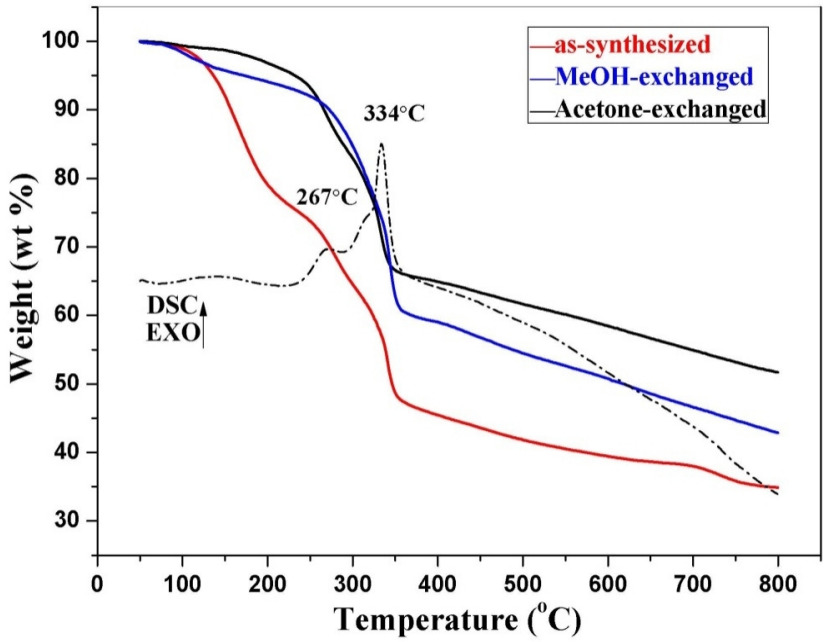


Figure S7. TG-DSC curves for the as-synthesized sample of **1** and samples after exchanged with methanol and acetone solvents.

Thermogravimetric analysis of as-synthesized sample of **1** showed a weight loss of 6.5 % up to 145 ºC, suggesting that the absorbed solvents (DMA and water) both in the surface and in the voids are evacuated at this temperature. To attain a more complete evacuation, DMA was exchanged with methanol or aceton by soaking crystals of **1** in methanol or aceton for 4 days, respectively. TGA results indicate that the acetone, as compared with methanol, is a better solvent for exchanging the higher boiling point solvents of DMA and water remained in the void of **1**. The TGA curve for the acetone-exchanged sample shows a weight loss of 0.8% between 50 and 150 ºC, corresponding to the evolution of guest solvent of acetone. A gradual further weight loss of 13.3% between 150 ºC and 280 ºC is corresponding to loss of 4 $[NC_2H_8]^+$ ions (ca. 13.7%). This process is in agreement with the small exothermic peak at 267 ºC. Further drastic weight loss from 280 ºC is corresponding to the loss of the BTT molecules and the collapse of the framework.

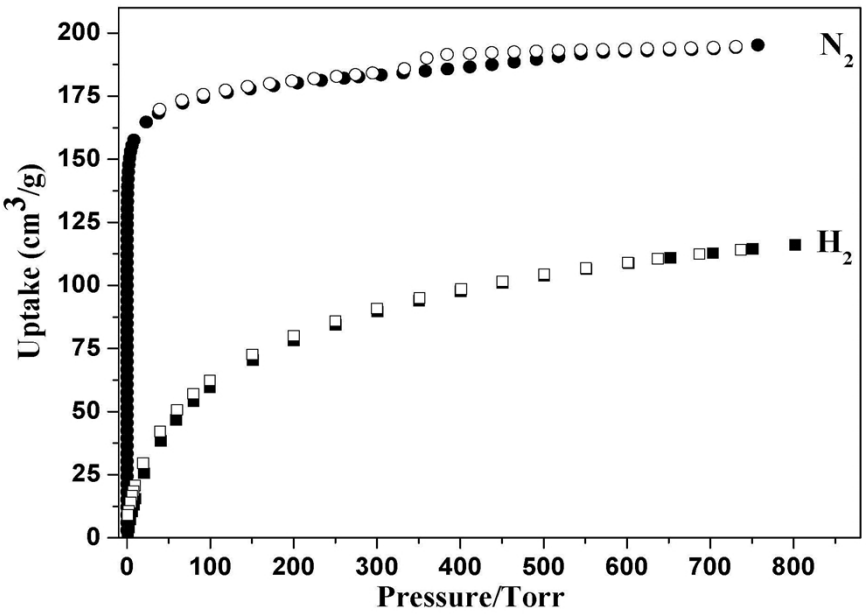


Figure S8. $N_2$ and $H_2$ sorption isotherms of **1a** at 77K, solid, adsorption; hollow, desorption.

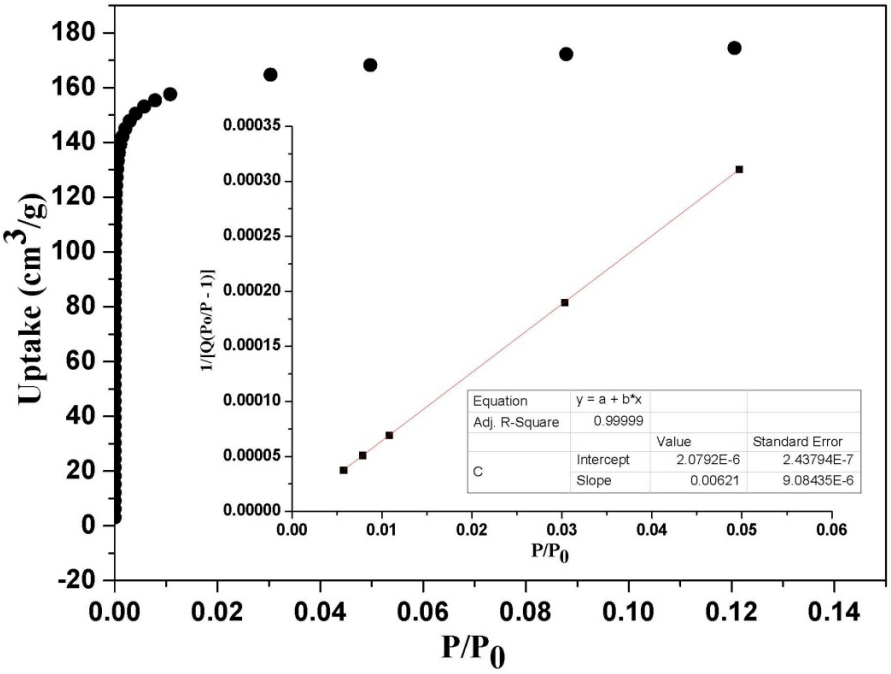


Figure S9. The plot of the linear region for the BET equation of **1a** ($P_0/P$= 0.005−0.05).

Table S5. Low-pressure $CO_2$ (273–298 K) or $H_2$ (77 K) adsorption capacities in selected metal-organic frameworks.

| MOFs | Pore Volume ($cm^3\ g^{-1}$) | Surface Area ($m^2/g$) | | Capacity[b]/$CO_2$ | | Capacity[b]/$H_2$ | |
|---|---|---|---|---|---|---|---|
| | | Langmuir | BET | 1 bar | Ref | 77 K | Ref |
| **1a** | 0.302 | 801 | 701 | 9.61 wt%, [a] 298 K<br>14.0 wt%,[a] 273 K | This work | 1.03 wt%,[a] 1 bar | This work |
| $Mg_2$(dobdc) | 0.573 | 2060 | 1800 | 26.7 wt%, 298 K | 13 | - | - |
| NTU-105 | 1.33 | - | 3543 | 26.8 wt%, 273 K | 14 | - | - |
| HKUST-1 | - | - | 1400 | 19.8 wt%, 293 K | 15 | - | - |
| SIFSIX-2-Cu-i | - | 821 | 735 | 19.2 wt%, 298 K | 16 | - | - |
| SIFSIX-1-Cu | 0.683 | - | 1468 | 18.5 wt%, 298 K | 17 | - | - |
| TIFSIX-1-Cu | 0.696 | - | 1690 | 17.3 wt%, 298 K | 17 | - | - |
| SNIFSIX-1-Cu | 0.636 | - | 1523 | 15.6 wt%, 298 K | 17 | - | - |
| mmen-Cu-BTTri | - | - | 870 | 15.4 wt%, 298 K | 18 | - | - |
| MPM-1-TIFSIX | - | - | 840 | 15.0 wt%, 298 K | 19 | - | - |
| Cu-BTTri | 0.713 | 1900 | 1770 | 14.3 wt%, 298 K | 20 | 1.7 wt%, 1.2 bar | 20 |
| Fe-BTT | - | - | 2010 | 13.5 wt%, 298 K | 21 | 2.3 wt% | 22 |
| CPF-6 | - | 883 | 599 | 16.1 wt%, 273 K | 23 | 1.85 wt% | 23 |
| SIFSIX-2-Cu | - | 3370 | 3140 | 7.5 wt%, 298 K | 16 | | |
| en-Cu-BTTri | - | 376 | 345 | 5.5 wt%, 298 K | 20 | - | - |
| MOF-177 | 1.89 | 5400 | 4690 | 3.6 wt%, 298 K | 13 | - | - |
| Mn-BTT | - | 2100 | 1100 | - | - | 2.1 wt% | 24 |
| Cu-BTT | - | - | 1710 | - | - | 2.3 wt% | 25 |

[a] Reported capacity was calculated from the excess adsorption.
[b] It was not clear from the reference whether the reported isotherms were in absolute or excess adsorption.

Table S6. Low-pressure (LP) and high-pressure (HP) gas sorption capacities of **1a** towards $CO_2$, $H_2$, $N_2$ and $CH_4$ at different temperatures.

| Gas | Pressure | 77 K | | | 273 K | | | 298 K | | |
|---|---|---|---|---|---|---|---|---|---|---|
| | | $cm^3/g$ | mol/Kg | wt% | $cm^3/g$ | mol/Kg | wt% | $cm^3/g$ | mol/Kg | wt%[a] |
| $CH_4$ | LP | - | | | 18.54 [a] | 0.83 [a] | 1.31 [a] | 10.62 [a] | 0.47 [a] | 0.75 [a] |
| $CO_2$ | LP | - | | | 82.80 [a] | 3.69 [a] | 14.0 [a] | 54.17 [a] | 2.42 [a] | 9.61 [a] |
| | HP | - | | | - | 5.76 [a] | 20.2 [a] | - | 5.30 [a] | 18.9 [a] |
| | | | | | - | 6.59 [b] | 22.5 [b] | - | 6.45 [b] | 22.1 [b] |
| | | | | | 30 bar | | | 45 bar | | |
| $N_2$ | LP | 195.3 [a] | 8.71 [a] | 19.6 [a] | 4.35 [a] | 0.19 [a] | 0.53 [a] | 2.60 [a] | 0.12 [a] | 0.33 [a] |
| | HP (65 bar) | - | | | - | 1.89 [a] | 5.03 [a] | - | 1.83 [a] | 4.87 [a] |
| | | | | | - | 2.87 [b] | 7.44 [b] | - | 2.72 [b] | 7.07 [b] |
| $H_2$ | LP | 116.1 [a] | 5.18 [a] | 1.03 [a] | 0.45 [a] | 0.02 [a] | 0.004 [a] | 0.228 [a] | 0.01 [a] | 0.002 [a] |
| | HP (65 bar) | - | | | - | 1.48 [a] | 0.30 [a] | - | 1.00 [a] | 0.2 [a] |
| | | | | | - | 2.32 [b] | 0.46 [b] | - | 1.77 [b] | 0.35 [b] |

In this work, wt% is defined as:

$$\text{wt}\,\% = \frac{\text{mass gas absobed}}{(\text{mass adsorbent} + \text{mass gas absorbed})} \times 100\,\%$$

[a] excess adsorption

[b] total adsorption

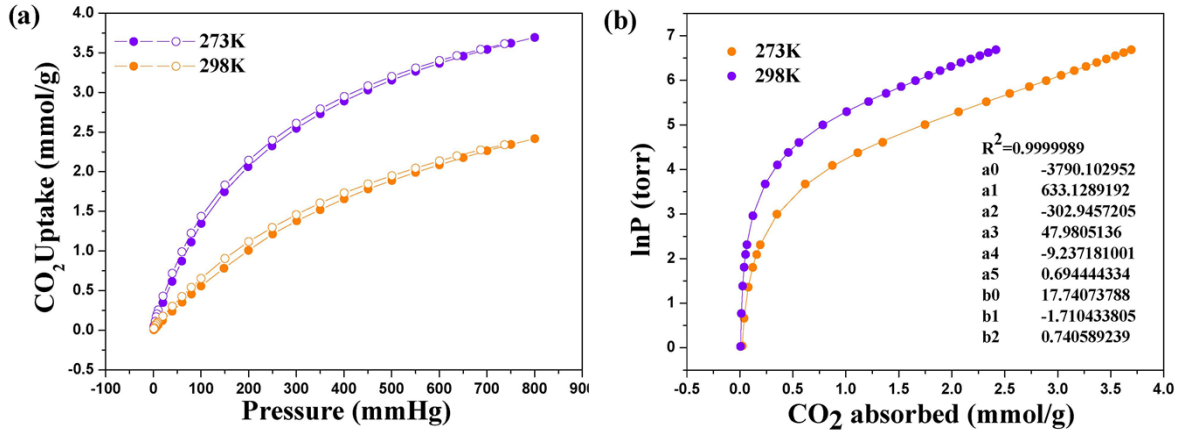


Figure S10. Virial fitting for $CO_2$ isotherms of **1a**: (a) The $CO_2$ adsorption isotherms for **1a** (solid circle, adsorption; hollow circle, desorption); (b) The details of virial equation (solid lines) fitting to the experimental $CO_2$ adsorption data (symbols) for **1a**.

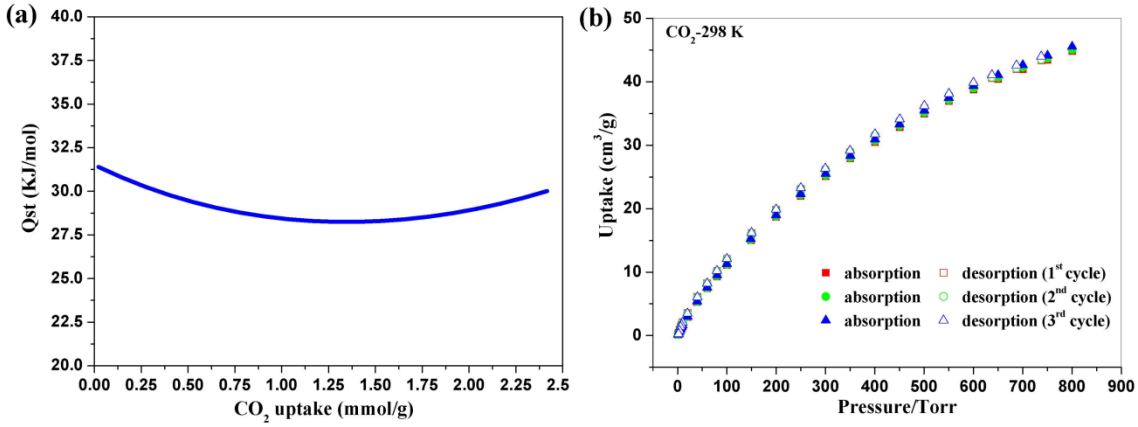


Figure S11. (a) The $CO_2$ adsorption enthalpy of **1a**; (b) $CO_2$ sorption isotherms of **1a** of three consecutive cycles.

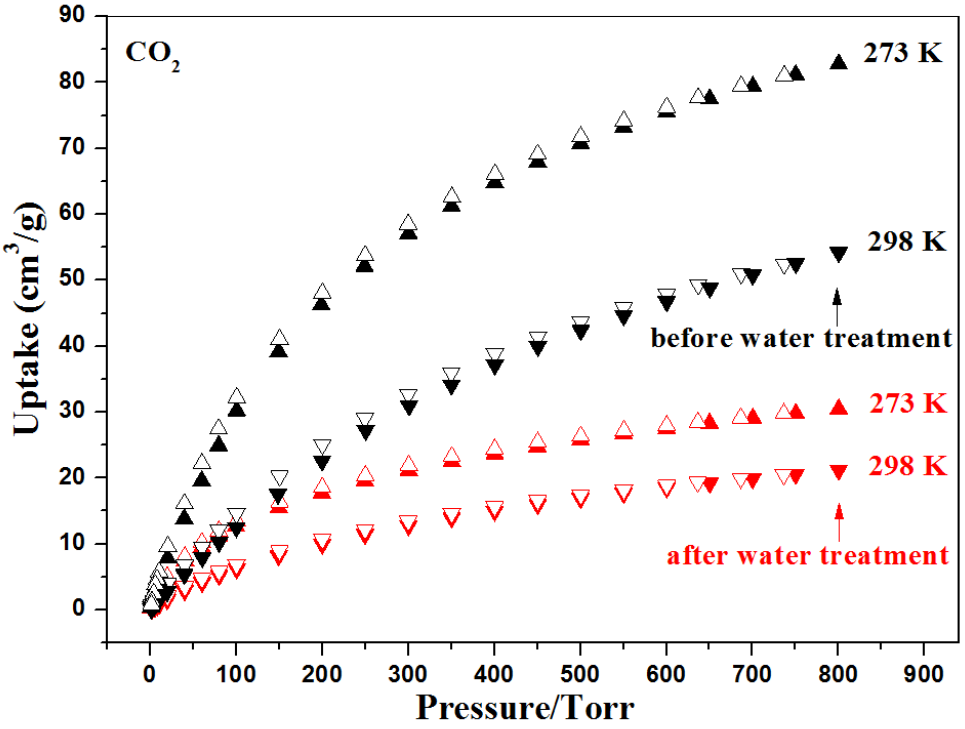


Figure S12. Comparisons of $CO_2$ uptakes before and after water treatment (immersion in liquid water for 1 day) at 273 and 298 K.

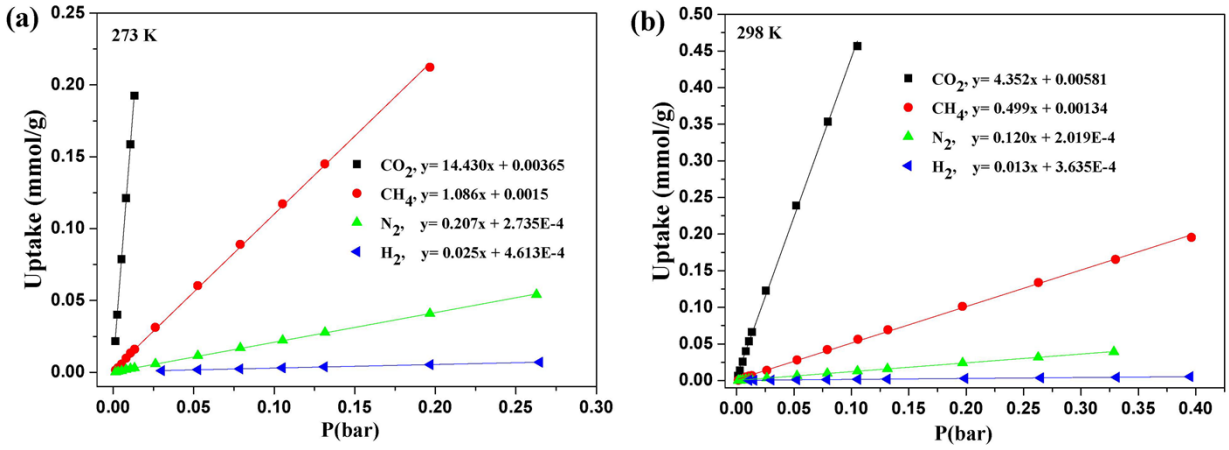


Figure S13. Low-pressure $CO_2/N_2$, $CO_2/CH_4$ and $CO_2/H_2$ initial slope selectivity studies for **1a** at 273 K (a) and 298 K (b).

Table S7. Low-pressure $CO_2/N_2$, $CO_2/CH_4$ and $CO_2/H_2$ selectivity results for **1a** analyzed by the initial slope ratio.

| | $CO_2/N_2$ selectivity | | $CO_2/H_2$ selectivity | | $CO_2/CH_4$ selectivity | |
|---|---|---|---|---|---|---|
| 273 K | 69.7 | 98.6% | 577.2 | 99.8% | 13.3 | 93.0% |
| 298 K | 36.3 | 97.3% | 334.8 | 99.7% | 8.7 | 89.7% |

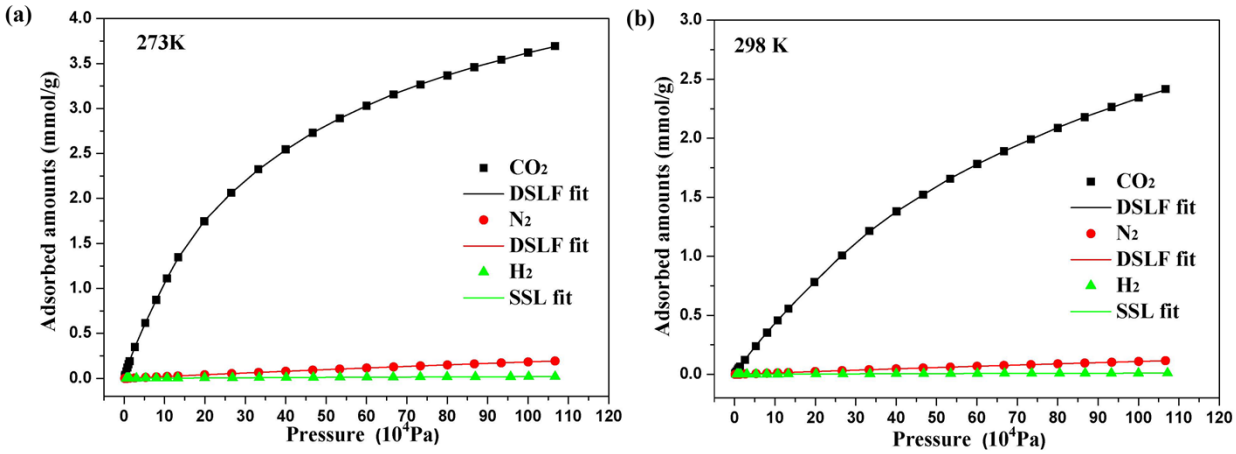


Figure S14. Low-pressure adsorption isotherms of $CO_2$, $H_2$ and $N_2$ at 273 K (a) and 298 K (b). Lines are fits to a dual-site Langmuir-Freundlich (DSLF) or single-site Langmuir (SSL) equation.

Table S8. The refined parameters for the DSLF and SSL equations fit for the pure isotherms of $CO_2$, $N_2$ and $H_2$ in **1a** at 273 K.

| | $CO_2$ | $H_2$ | | $N_2$ |
|---|---|---|---|---|
| $R^2$ | 0.999997 | 0.999709 | $R^2$ | 0.999991 |
| $q_{m,1}$ | 5.290562 | 0.047092 | $q_m$ | 1.408277 |
| $q_{m,2}$ | 0.140931 | 4.522968E-2 | b | 1.496390E-6 |
| $b_1$ | 5.292282E-5 | 2.876264E-6 | | |
| $b_2$ | 7.554743E-21 | 9.558976E-9 | | |
| $n_1$ | 1.096608 | 0.932293 | | |
| $n_2$ | 0.200848 | 0.380865 | | |

Table S9. The refined parameters for the DSLF and SSL equations fit for the pure isotherms of $CO_2$, $N_2$ and $H_2$ in **1a** at 298 K.

| | $CO_2$ | $H_2$ | | $N_2$ |
|---|---|---|---|---|
| $R^2$ | 0.999993 | 0.999537 | $R^2$ | 0.999992 |
| $q_{m,1}$ | 4.639673 | 0.007053 | $q_m$ | 0.962695 |
| $q_{m,2}$ | 0.061961 | 0.006664 | b | 1.282220E-6 |
| $b_1$ | 1309095E-5 | 8.654679E-12 | | |
| $b_2$ | 3.200345E-32 | 1.671942E-4 | | |
| $n_1$ | 1.027170 | 0.431704 | | |
| $n_2$ | 0.139846 | 1.219561 | | |

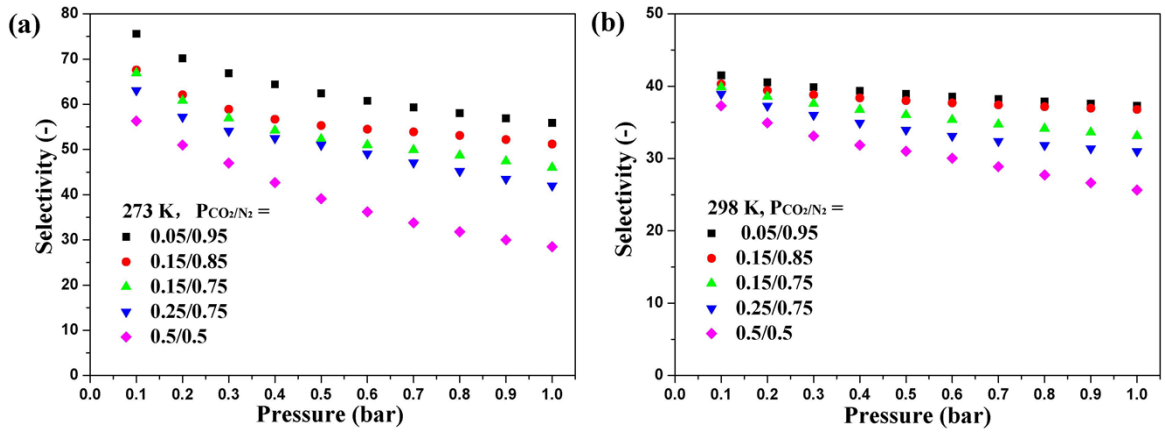


Figure S15. IAST selectivities of $CO_2$ over $N_2$ in **1a** at different mixture composition at 273 K (a) and 298 K (b).

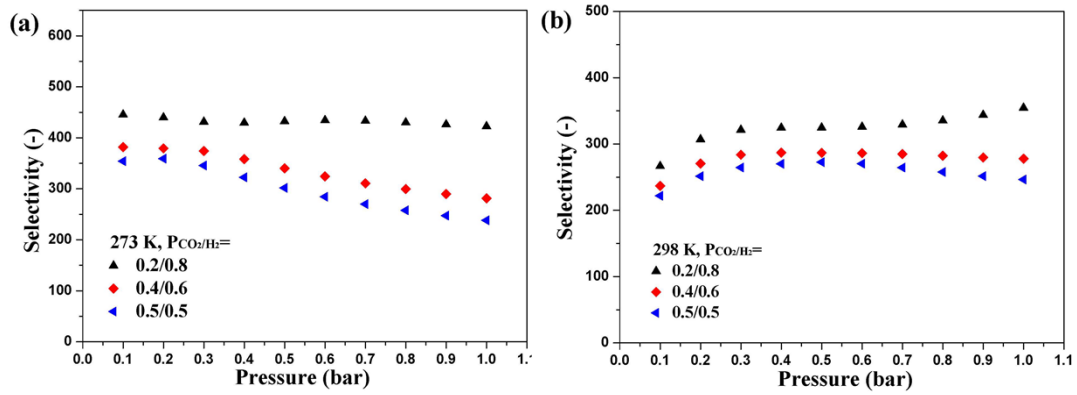


Figure S16. IAST selectivites of $CO_2$ over $H_2$ in **1a** at different mixture compositions as a function of total pressure at 273 K (a) and 298 K (b).

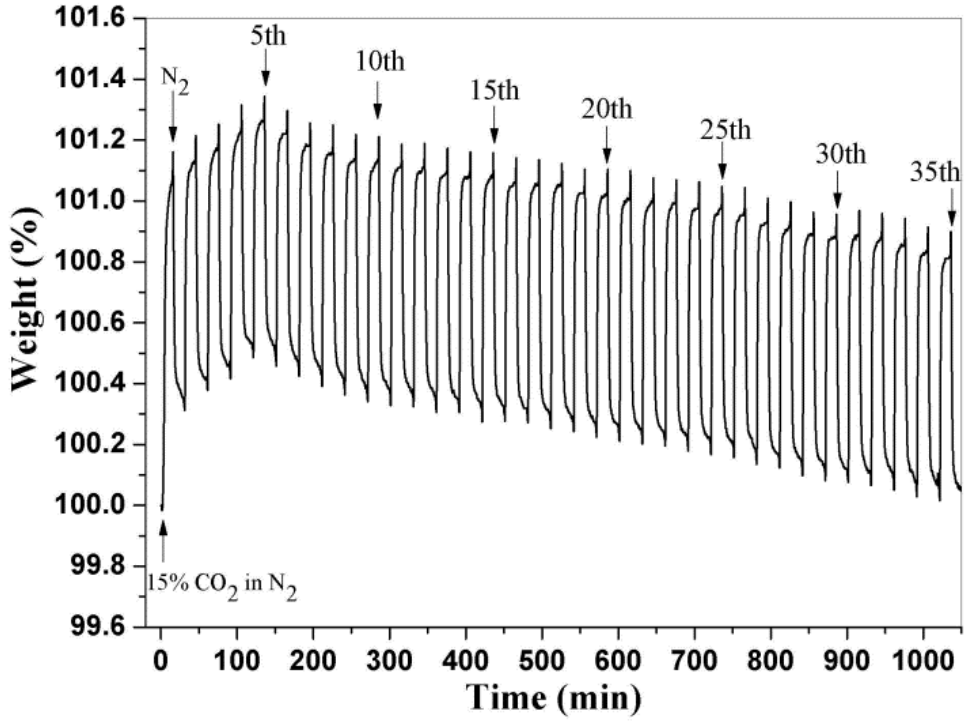


Figure S17. Gas cycling experiment for 1a under a mixed $CO_2$–$N_2$ (15:85 v/v) flow and a pure $N_2$ flow at a constant temperature of 303 K for 35 cycles.

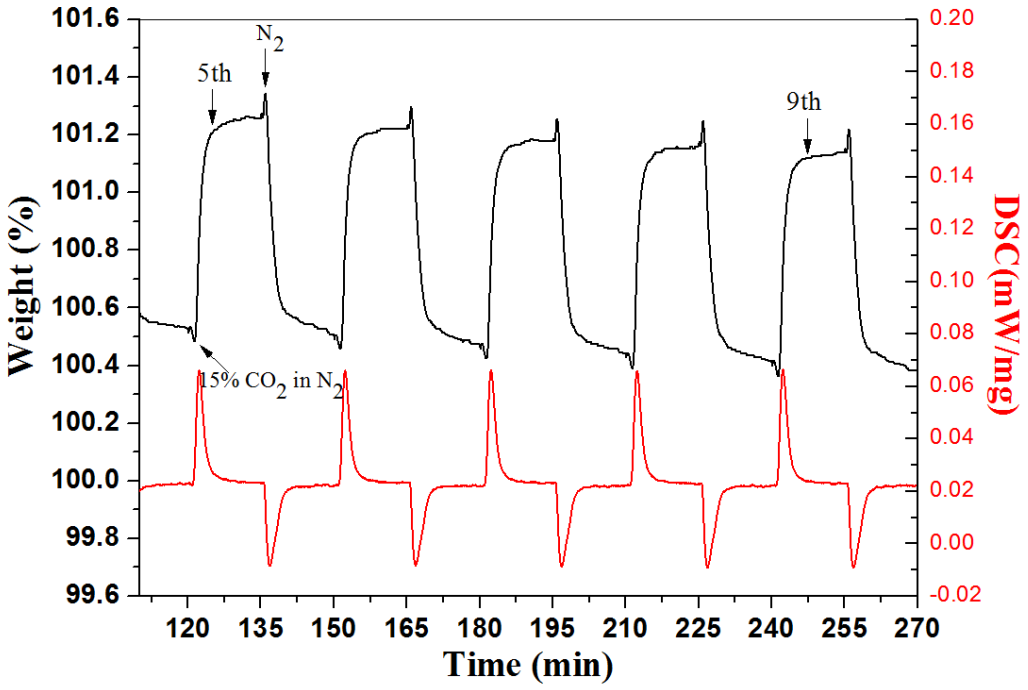


Figure S18. An enlargment of five cycles—TG-DSC curves from cycle 5$^{th}$ to cycle 9$^{th}$.

The flow rates for pure $N_2$ gas and $CO_2$–$N_2$ (15:85 v/v) mixture gas are 60 mL min$^{-1}$ and 40 mL min$^{-1}$, respectively.

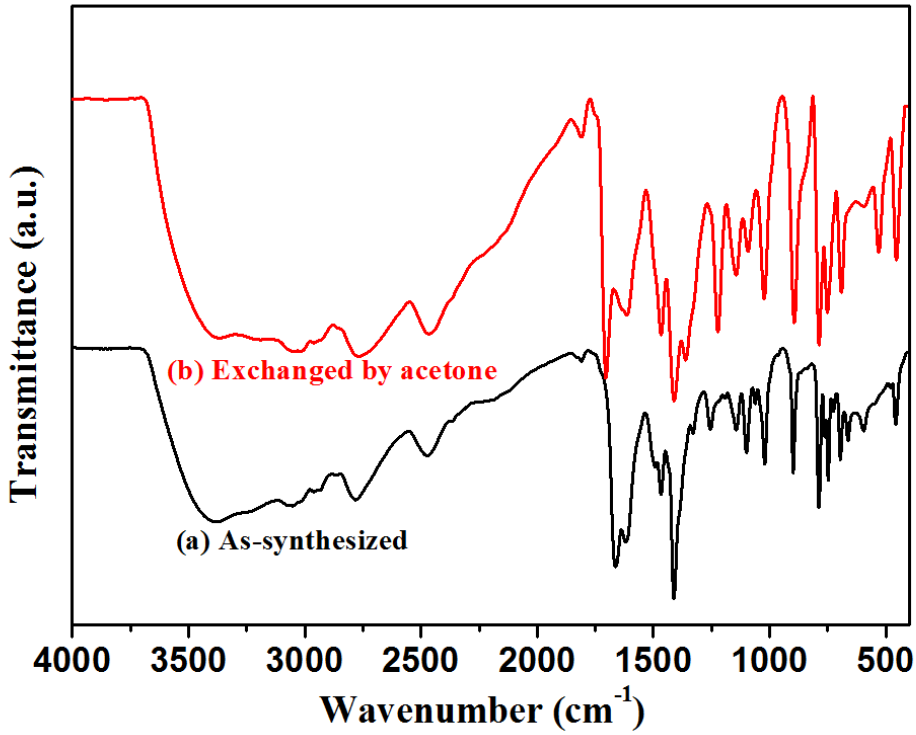


Figure S19. The IR spectra of the as-synthesized sample (a) and acetone-exchanged one (b).

Table S10. The weight change for the special cycle in the gas cycling experiment.

| Cycle | 2nd | 5th | 10th | 15th | 20th | 25th | 30th | 35th |
|---|---|---|---|---|---|---|---|---|
| Weight change (wt%) | 0.8 | 0.73 | 0.75 | 0.76 | 0.75 | 0.75 | 0.75 | 0.74 |

Table S11. High-pressure excess sorption and total sorption data of **1a**.

| $CO_2$ at 273K | | | | |
|---|---|---|---|---|
| P (bar) | Excess Uptake (%) | Total Uptake (%) | Excess Uptake (mmol/g) | Total Uptake (mmol/g) |
| 0.019 | 2.24709 | 2.248202 | 0.52244 | 0.522706 |

| | | | | |
|---|---|---|---|---|
| 0.218 | 7.58666 | 7.59943 | 1.86579 | 1.869191 |
| 0.417 | 10.0336 | 10.05806 | 2.53468 | 2.541553 |
| 0.619 | 11.52851 | 11.56474 | 2.96154 | 2.97206 |
| 0.817 | 12.52434 | 12.57233 | 3.25398 | 3.268243 |
| 1.418 | 14.30794 | 14.39152 | 3.79476 | 3.820651 |
| 2.9179 | 16.23063 | 16.40458 | 4.40349 | 4.45995 |
| 5.9194 | 17.732 | 18.09159 | 4.89862 | 5.019907 |
| 9.9176 | 18.63566 | 19.25542 | 5.20545 | 5.419848 |
| 13.9188 | 19.19078 | 20.08776 | 5.39733 | 5.713016 |
| 17.9184 | 19.52486 | 20.71903 | 5.51408 | 5.939472 |
| 22.8337 | 19.8205 | 21.41577 | 5.61822 | 6.193637 |
| 27.8341 | 20.07605 | 22.13412 | 5.70885 | 6.460444 |
| 29.8341 | 20.21935 | 22.48383 | 5.75993 | 6.592122 |
| 26.0268 | 20.03147 | 21.9157 | 5.693 | 6.378801 |
| 22.0299 | 19.82394 | 21.35044 | 5.61943 | 6.169613 |
| 19.0329 | 19.66084 | 20.9422 | 5.56189 | 6.020395 |
| 15.0325 | 19.35676 | 20.33375 | 5.45522 | 5.800836 |
| 12.0318 | 19.02822 | 19.79184 | 5.34087 | 5.60809 |
| 9.0312 | 18.58693 | 19.1476 | 5.18873 | 5.382312 |
| 7.029 | 18.1587 | 18.589 | 5.04266 | 5.189438 |
| 5.0348 | 17.5034 | 17.80749 | 4.82207 | 4.923998 |
| 2.536 | 15.98438 | 16.13515 | 4.32397 | 4.372607 |
| 1.2374 | 13.97763 | 14.05066 | 3.69292 | 3.715365 |

| $CO_2$ at 298K | | | | |
|---|---|---|---|---|
| P (bar) | Excess Uptake (%) | Total Uptake (%) | Excess Uptake (mmol/g) | Total Uptake (mmol/g) |
| 0.018 | 0.68444 | 0.685405 | 0.15663 | 0.156849 |
| 0.22 | 3.55136 | 3.563171 | 0.83685 | 0.839733 |
| 0.617 | 6.84884 | 6.882049 | 1.671 | 1.6797 |
| 1.117 | 9.10571 | 9.165772 | 2.2768 | 2.293332 |
| 1.918 | 11.14969 | 11.25347 | 2.85201 | 2.881923 |
| 3.917 | 13.62753 | 13.84149 | 3.58583 | 3.65117 |
| 6.9215 | 15.29985 | 15.68312 | 4.10535 | 4.227322 |
| 9.9203 | 16.22361 | 16.7813 | 4.40122 | 4.583021 |
| 14.92 | 17.10881 | 17.96959 | 4.69093 | 4.978637 |
| 19.9215 | 17.68845 | 18.87083 | 4.88401 | 5.286414 |
| 24.8354 | 18.06204 | 19.58093 | 5.0099 | 5.533775 |
| 29.836 | 18.37208 | 20.25951 | 5.11525 | 5.774274 |
| 34.8338 | 18.60694 | 20.89449 | 5.19559 | 6.003056 |
| 39.8337 | 18.78761 | 21.51605 | 5.25771 | 6.230589 |
| 44.6492 | 18.91377 | 22.11849 | 5.30125 | 6.454588 |

| | | | | |
|---|---|---|---|---|
| 38.0328 | 18.75359 | 21.31774 | 5.24599 | 6.157602 |
| 33.032 | 18.54064 | 20.67976 | 5.17287 | 5.925278 |
| 28.0309 | 18.31642 | 20.06761 | 5.09628 | 5.705848 |
| 23.032 | 17.9841 | 19.37688 | 4.98354 | 5.462251 |
| 18.0307 | 17.55996 | 18.61832 | 4.84097 | 5.199496 |
| 13.0324 | 16.89391 | 17.63819 | 4.62003 | 4.86716 |
| 9.0316 | 16.1128 | 16.6182 | 4.36539 | 4.529601 |
| 5.0336 | 14.58749 | 14.86366 | 3.88156 | 3.967876 |
| 3.036 | 13.06458 | 13.2298 | 3.41543 | 3.465214 |

| $H_2$ at 273K | | | | |
|---|---|---|---|---|
| P (bar) | Excess Uptake (%) | Total Uptake (%) | Excess Uptake (mmol/g) | Total Uptake (mmol/g) |
| 0.185 | 0.08061 | 8.11E-02 | 0.40337 | 4.06E-01 |
| 0.38 | 0.08267 | 0.083688 | 0.41367 | 0.418792 |
| 0.7298 | 0.08618 | 0.088135 | 0.43126 | 0.441066 |
| 0.981 | 0.09431 | 0.096939 | 0.47198 | 0.485165 |
| 4.02 | 0.11097 | 0.121723 | 0.55546 | 0.609355 |
| 6.9763 | 0.12513 | 0.143755 | 0.62643 | 0.719811 |
| 9.9868 | 0.14119 | 0.167792 | 0.70694 | 0.840371 |
| 11.944 | 0.15354 | 0.185316 | 0.76889 | 0.9283 |
| 14.9388 | 0.16743 | 0.207098 | 0.83854 | 1.037638 |
| 17.9513 | 0.18461 | 0.232203 | 0.92474 | 1.163717 |
| 19.9454 | 0.19314 | 0.245953 | 0.96755 | 1.232795 |
| 24.8406 | 0.21214 | 0.277685 | 1.06296 | 1.392292 |
| 29.8346 | 0.22719 | 0.30569 | 1.13852 | 1.533135 |
| 34.8627 | 0.23726 | 0.328694 | 1.18911 | 1.648891 |
| 39.8735 | 0.25441 | 0.35865 | 1.27527 | 1.799704 |
| 44.698 | 0.26228 | 0.37877 | 1.31483 | 1.901053 |
| 49.6993 | 0.28148 | 0.410588 | 1.41137 | 2.061405 |
| 54.6696 | 0.28227 | 0.423785 | 1.41536 | 2.127943 |
| 59.6921 | 0.29115 | 0.445221 | 1.45999 | 2.236063 |
| 64.6707 | 0.29532 | 0.461647 | 1.48098 | 2.318939 |
| 69.6691 | 0.30577 | 0.484438 | 1.53353 | 2.433983 |
| 63.0292 | 0.303 | 0.465277 | 1.51959 | 2.337259 |
| 58.0034 | 0.29489 | 0.444766 | 1.47881 | 2.233765 |
| 53.0227 | 0.28211 | 0.419508 | 1.41454 | 2.106375 |
| 48.0099 | 0.27089 | 0.395745 | 1.35815 | 1.986589 |
| 43.0021 | 0.25951 | 0.371663 | 1.30094 | 1.865245 |
| 38.0077 | 0.24144 | 0.340886 | 1.21011 | 1.710258 |
| 33.0271 | 0.22656 | 0.313251 | 1.13537 | 1.571175 |
| 28.0111 | 0.20659 | 0.280351 | 1.03507 | 1.405697 |

| | | | | |
|---|---|---|---|---|
| 23.0134 | 0.1868 | 0.247639 | 0.93574 | 1.241269 |
| 19.0176 | 0.16712 | 0.217487 | 0.83702 | 1.089807 |
| 13.0284 | 0.14896 | 0.183597 | 0.74589 | 0.919674 |
| 8.0299 | 0.12528 | 0.146696 | 0.62718 | 0.734558 |
| 3.035 | 0.10365 | 0.11177 | 0.51878 | 0.559476 |
| 1.2352 | 0.08782 | 0.091129 | 0.4395 | 0.456058 |

| $H_2$ at 298K | | | | |
|---|---|---|---|---|
| P (bar) | Excess Uptake (%) | Total Uptake (%) | Excess Uptake (mmol/g) | Total Uptake (mmol/g) |
| 0.191 | 0.05727 | 0.057739 | 0.28649 | 0.288863 |
| 0.389 | 0.06787 | 0.068825 | 0.33959 | 0.344364 |
| 0.697 | 0.06582 | 0.067532 | 0.32934 | 0.337886 |
| 1.002 | 0.07034 | 0.0728 | 0.35196 | 0.364266 |
| 4.019 | 0.08168 | 0.09153 | 0.40872 | 0.458067 |
| 6.9517 | 0.09361 | 0.110617 | 0.4685 | 0.553696 |
| 9.944 | 0.10365 | 0.127933 | 0.51881 | 0.640485 |
| 11.9645 | 0.11405 | 0.143241 | 0.57088 | 0.717234 |
| 14.9398 | 0.12533 | 0.161859 | 0.62743 | 0.810605 |
| 17.9465 | 0.13014 | 0.173911 | 0.65155 | 0.871069 |
| 19.9516 | 0.13959 | 0.187887 | 0.69895 | 0.941202 |
| 24.858 | 0.15017 | 0.210232 | 0.752 | 1.053374 |
| 29.8578 | 0.15812 | 0.230246 | 0.79184 | 1.153886 |
| 34.8792 | 0.17058 | 0.254466 | 0.85437 | 1.275574 |
| 39.8694 | 0.17091 | 0.266552 | 0.85599 | 1.336324 |
| 44.6804 | 0.18471 | 0.291504 | 0.92526 | 1.46178 |
| 49.684 | 0.18655 | 0.305095 | 0.9345 | 1.530145 |
| 54.7093 | 0.19144 | 0.321433 | 0.95906 | 1.612347 |
| 59.6895 | 0.19381 | 0.335248 | 0.97094 | 1.681877 |
| 64.7093 | 0.19933 | 0.35221 | 0.99866 | 1.767274 |
| 69.6753 | 0.20551 | 0.369529 | 1.02967 | 1.854496 |
| 62.9699 | 0.19898 | 0.347946 | 0.99688 | 1.745803 |
| 58.0078 | 0.19337 | 0.330893 | 0.9687 | 1.659956 |
| 52.9969 | 0.17856 | 0.304637 | 0.8944 | 1.527839 |
| 47.9967 | 0.17033 | 0.284958 | 0.85309 | 1.428864 |
| 43.0217 | 0.15121 | 0.254086 | 0.7572 | 1.273666 |
| 38.0003 | 0.13698 | 0.228101 | 0.68585 | 1.143112 |
| 33.0108 | 0.1215 | 0.200863 | 0.60825 | 1.006336 |
| 28.0119 | 0.11042 | 0.178022 | 0.55272 | 0.891699 |
| 23.0204 | 0.09841 | 0.154249 | 0.49256 | 0.772435 |
| 19.0202 | 0.09378 | 0.139965 | 0.46935 | 0.700804 |
| 13.0288 | 0.07519 | 0.10689 | 0.37621 | 0.535022 |

| | | | | |
|---|---|---|---|---|
| 8.0306 | 0.06701 | 0.086643 | 0.33528 | 0.433592 |
| 3.0355 | 0.05192 | 0.059366 | 0.25973 | 0.297007 |
| 1.2355 | 0.05634 | 0.059373 | 0.28186 | 0.297041 |

| $N_2$ at 273K | | | | |
|---|---|---|---|---|
| P (bar) | Excess Uptake (%) | Total Uptake (%) | Excess Uptake (mmol/g) | Total Uptake (mmol/g) |
| 0.22 | 0.0661 | 0.074301 | 0.02362 | 2.66E-02 |
| 0.6267 | 0.24688 | 0.270243 | 0.08839 | 9.68E-02 |
| 0.936 | 0.3735 | 0.40852 | 0.13389 | 1.46E-01 |
| 2.927 | 1.08293 | 1.192135 | 0.39099 | 4.31E-01 |
| 6.9261 | 2.07704 | 2.335486 | 0.75753 | 8.54E-01 |
| 9.9181 | 2.61324 | 2.98E+00 | 0.95834 | 1.10E+00 |
| 14.9282 | 3.24337 | 3.80016 | 1.19718 | 1.41E+00 |
| 19.9191 | 3.6513 | 4.394097 | 1.35346 | 1.64E+00 |
| 24.8392 | 4.01526 | 4.941887 | 1.49401 | 1.86E+00 |
| 29.838 | 4.24981 | 5.362246 | 1.58516 | 2.02E+00 |
| 34.8404 | 4.42817 | 5.725718 | 1.65477 | 2.17E+00 |
| 39.8415 | 4.61009 | 6.094111 | 1.72603 | 2.32E+00 |
| 49.6761 | 4.82807 | 6.674494 | 1.81179 | 2.55E+00 |
| 59.6663 | 5.00386 | 7.21725 | 1.88123 | 2.78E+00 |
| 65.0238 | 5.03202 | 7.439373 | 1.89237 | 2.87E+00 |
| 55.0196 | 4.92074 | 6.964033 | 1.84836 | 2.67E+00 |
| 45.0284 | 4.73839 | 6.412852 | 1.77646 | 2.45E+00 |
| 38.0288 | 4.51402 | 5.929701 | 1.68836 | 2.25E+00 |
| 33.0258 | 4.39183 | 5.621957 | 1.64056 | 2.13E+00 |
| 28.0247 | 4.1819 | 5.227253 | 1.55872 | 1.97E+00 |
| 23.0323 | 3.87654 | 4.735239 | 1.44031 | 1.78E+00 |
| 18.0314 | 3.52028 | 4.192512 | 1.30312 | 1.56E+00 |
| 13.033 | 3.03767 | 3.523631 | 1.11887 | 1.30E+00 |
| 8.0304 | 2.29223 | 2.59182 | 0.83786 | 9.50E-01 |
| 5.0337 | 1.68411 | 1.871903 | 0.61177 | 6.81E-01 |
| 2.536 | 0.96393 | 1.058367 | 0.34761 | 3.82E-01 |
| 1.2358 | 0.50087 | 0.547055 | 0.17978 | 1.96E-01 |

| $N_2$ at 298K | | | | |
|---|---|---|---|---|
| P (bar) | Excess Uptake (%) | Total Uptake (%) | Excess Uptake (mmol/g) | Total Uptake (mmol/g) |
| 0.223 | 0.03731 | 4.49E-02 | 0.01333 | 0.016052 |
| 0.624 | 0.18581 | 0.207125 | 0.06649 | 0.074127 |

| | | | | |
|---|---|---|---|---|
| 0.926 | 0.28666 | 0.31836 | 0.10267 | 0.114063 |
| 2.936 | 0.93524 | 1.035404 | 0.33717 | 0.373656 |
| 6.9181 | 1.87834 | 2.114248 | 0.68368 | 0.771398 |
| 9.9208 | 2.35038 | 2.68868 | 0.85963 | 0.986774 |
| 14.9237 | 2.96945 | 3.477836 | 1.09297 | 1.286839 |
| 19.9236 | 3.37648 | 4.054671 | 1.24802 | 1.509294 |
| 24.8382 | 3.70286 | 4.547011 | 1.3733 | 1.701291 |
| 29.8436 | 4.01946 | 5.032569 | 1.49564 | 1.892592 |
| 34.8403 | 4.23522 | 5.415827 | 1.57947 | 2.044976 |
| 39.84 | 4.42671 | 5.775131 | 1.6542 | 2.188962 |
| 49.672 | 4.72126 | 6.396014 | 1.76972 | 2.440378 |
| 59.6682 | 4.91875 | 6.923486 | 1.84758 | 2.656603 |
| 65.0157 | 4.88615 | 7.065452 | 1.8347 | 2.715218 |
| 55.0238 | 4.66021 | 6.513034 | 1.74571 | 2.488137 |
| 45.0267 | 4.3059 | 5.827131 | 1.60702 | 2.209892 |
| 38.0246 | 4.07147 | 5.359308 | 1.51581 | 2.022427 |
| 33.0301 | 3.8126 | 4.933304 | 1.41561 | 1.853324 |
| 28.0302 | 3.54217 | 4.49458 | 1.31152 | 1.68075 |
| 23.0307 | 3.16898 | 3.952522 | 1.16882 | 1.469705 |
| 18.0277 | 2.8265 | 3.440598 | 1.03883 | 1.272569 |
| 13.0317 | 2.27244 | 2.716813 | 0.83046 | 0.997387 |
| 8.0304 | 1.63138 | 1.905447 | 0.5923 | 0.693735 |
| 5.032 | 1.13161 | 1.303454 | 0.40877 | 0.471667 |
| 2.536 | 0.59947 | 0.686069 | 0.21539 | 0.246717 |
| 1.2358 | 0.30692 | 0.349182 | 0.10995 | 0.125145 |

# References.


1 M. Hill, M. F. Mahon, K. C. Molloy, *J. Chem. Soc. Dalton Trans*., 1996, **9**, 1857.

2 G. M. Sheldrick, *Acta Crystallogr. Sect. A.,* 2008, **64**, 112.

3 A. L. Spek, *J. Appl. Crystallogr*., 2003, **36**, 7.

4 *(a)* J. Rouquerol, P. Llewellyn, F. Rouquerol, *Stud. Surf. Sci. Catal*., 2007, **160**, 49; *(b)* K. S. Walton, R. Q. Snurr, *J. Am. Chem. Soc*., 2007, **129**, 8552.

5 S. Hong, M. Oh, M. Park, J. W. Yoon, J. S. Chang, M. S. Lah, *Chem. Commun*., 2009, **36**, 5397.

6 *(a)* S. S. Kaye, A. Dailly, O. M. Yaghi, J. R. Long, *J. Am. Chem. Soc*., 2007, **129**, 14176; *(b)* H. Furukawa, M. A. Miller, O. M. Yaghi, *J. Mater. Chem*., 2007, **17**, 3197; *(c)* A. R. Millward, O. M. Yaghi, *J. Am. Chem. Soc*., 2005, **127**, 17998; *(d)* L.-J. Li, J. G. Bell, S.-F. Tang, X.-X. Lv, C. Wang, Y.-L. Xing, X.-B. Zhao, K. M. Thomas, *Chem. Mater*., 2014, **26**, 4679.

7 NIST Chemistry WebBook (Thermophysical Properties of Fluid Systems): http:// webbook.nist.gov/chemistry/fluid/.

8 J. L. C. Rowsell, O. M. Yaghi, *J. Am. Chem. Soc*., 2006, **128**, 1304.

9 *(a)* A. L. Myers, J. M. Prausnitz, *AIChE J*., 1965, **11**, 121; *(b)* Y. S. Bae, K. L. Mulfort, H. Frost, P. S. Ryan, Broadbelt, L. J. Punnathanam, J. T. Hupp, R. Q. Snurr, *Langmuir*, 2008, **24,** 8592; *(c)* B. Mu, F. Li, K. S. Walton, *Chem. Commun*., 2009, **18**, 2493.

10 J. A. Mason, K. Sumida, Z. R. Herm, R. Krishna, J. R. Long, *Energy Environ*. Sci., 2011, **4**, 3030.

11 Y.-B. He, Z.-J. Zhang, S.-C. Xiang, F. R. Fronczek, R. Krishna, B.-L. Chen, *Chem. Commun*., 2012, **48**, 6493.

12 B.-S. Zheng, J.-F. Bai, J.-G. Duan, L. Wojtas, M. J. Zaworotko, *J. Am. Chem. Soc*., 2011, **133**, 748.

13 Z. R. Herm, J. A. Swisher, B. Smit, R. Krishna, J. R. Long, *J. Am. Chem. Soc.,* 2011, **133**, 5664.

14 X.-J. Wang, P.-Z. Li, Y.-F. Chen, Q. Zhang, H.-C. Zhang, X.-X. Chan, R. Ganguly, Y.-X. Li, J.-W. Jiang, Y.-L. Zhao, *Sci Rep.,* 2013, **3**, 1149.

15 P. Aprea, D. Caputo, N. Gargiulo, F. Iucolano, F. Pepe, *J. Chem. Eng. Data.,* 2010, **55**, 3655.

16 P. Nugent, Y. Belmabkhout, S. D. Burd, A. J. Cairns, R. Luebke, K. Forrest, T. Pham, S. Q. Ma, B. Space, L, Wojtas, M. Eddaoudi, M. J. Zaworotko, *Nature*, 2013, **495**, 80.

17 P. Nugent, V. Rhodus, T. Pham, B. Tudor, K. Forrest, L, Wojtas, B. Space, M. J. Zaworotko, *Chem. Commun*., 2013, **49**, 1606.

18 T. M. McDonald, D. M. D'Alessandro, R. Krishna, J. R. Long, *Chem. Sci.,* 2011, **2**, 2022.

19 P. Nugent, V. L. Rhodus, T. Pham, K. Forrest, L. Wojtas, B. Space, M. J. Zaworotko, *J. Am. Chem. Soc.*, 2013, **135**, 10950.

20 A. Demessence, D. M. D'Alessandro, M. L. Foo, J. R. Long, *J. Am. Chem. Soc.,* 2009, **131**, 8784.

21 K. Sumida, S. Horike, S. S. Kaye, Z. R. Herm, W. L. Queen, C. M. Brown, F. Grandjean, G. J. Long, A. Dailly, J. R. Long, *Chem. Sci.,* 2010, **1**, 184.

22 K. Sumida, D. Stück, L. Mino, J. D. Chai, E. D. Bloch, O. Zavorotynska, L. J. Murray, M. Dincă, S. Chavan, S. Bordiga, M. Head-Gordon, J. R. Long, *J. Am. Chem. Soc.,* 2013, **135**, 1083.

23 Q.-P. Lin, T. Wu, S.-T. Zheng, X.-H. Bu, P.-Y. Feng, *J. Am. Chem.Soc.,* 2012, **134**, 784.

24 M. Dincă, A. Dailly, Y. Liu, C. M. Brown, D. A. Neumann, J. R. Long, *J. Am. Chem. Soc.,* 2006, **128**, 16876.

25 M. Dincă, W. S. Han, Y. Liu, A. Dailly, C. M. Brown, J. R. Long, *Angew. Chem. Int. Ed.,* 2007, **46**, 1419.